Co-active receptor tyrosine kinases mitigate the effect of FGFR inhibitors in *FGFR1*-amplified lung cancers with low FGFR1 protein expression

Hiroshi Kotani[1,5], Hiromichi Ebi[1,5], Hidenori Kitai[1], Shigeki Nanjo[1], Kenji Kita[1], Tiffany G. Huynh[2], Akishi Ooi[3], Anthony C. Faber[4], Mari Mino-Kenudson[2], Seiji Yano[1]

1. Division of Medical Oncology, Cancer Research Institute, Kanazawa University, Ishikawa 920-8641, Japan
2. Department of Pathology, Massachusetts General Hospital, 55 Fruit Street, Warren 122, Boston, MA 02114, USA
3. Department of Molecular and Cellular Pathology, Graduate School of Medical Science, Kanazawa University, Ishikawa 920-8641, Japan
4. VCU Philips Institute for Oral Health Research, School of Dentistry and Massey Cancer Center, Virginia Commonwealth University, Richmond, VA, USA

5. These authors contributed equally to this work.

Corresponding Authors:

Hiromichi Ebi, MD, PhD

Division of Medical Oncology

Cancer Research Institute, Kanazawa University

13-1, Takaramachi, Kanazawa, Ishikawa, 920-0934, Japan

Phone: +81- 76-265-2794

Fax: +81- 76-244-2454

E-mail: hebi@staff.kanazawa-u.ac.jp

Seiji Yano, MD, PhD

Division of Medical Oncology

Cancer Research Institute, Kanazawa University

13-1, Takaramachi, Kanazawa, Ishikawa, 920-0934, Japan

Phone: +81- 76-265-2794

Fax: +81- 76-244-2454

E-mail: syano@staff.kanazawa-u.ac.jp

Running title: Co-drivers in *FGFR1*-amplified lung cancer

Conflict of interest: The authors declare no conflict of interest.

Financial support: This work is supported by Grants-in-Aid for Scientific Research (H. Ebi, 26830105; S. Yano, 21390256), Scientific Research on Innovative Areas "Integrative Research on Cancer Microenvironment Network" (S. Yano, 22112010A01), and Grant-in-Aid for Project for Development of Innovative Research on Cancer Therapeutics (P-Direct) from the Ministry of Education, Culture, Sports, Science, and Technology (MEXT) of Japan.

Word count: 4565

Total number of figures: 7

Total number of supplementary figures and tables: 4 supplementary figures and 4 supplementary tables.

Abstract

Targeted therapies are effective in subsets of lung cancers with *EGFR* mutations and *ALK* translocations. Large-scale genomics have recently expanded the lung cancer landscape with *FGFR1* amplification found in roughly 20% of squamous cell carcinomas (SCCs). However, the response rates have been low for biomarker-directed FGFR inhibitor therapy in SCC, which contrasts to the relatively high rates of response seen in *EGFR* mutant and *ALK* translocated lung cancers treated with EGFR inhibitors and ALK inhibitors, respectively. In order to better understand the low response rates of *FGFR1*-amplified lung cancers to FGFR inhibitors, relationships between gene copy number, mRNA expression, and protein expression of FGFR1 were assessed in cell lines, tumor specimens, and data from The Cancer Genome Atlas (TCGA). The importance of these factors for the sensitivity to FGFR inhibitors was determined by analyzing drug screen data and conducting in vitro and in vivo experiments. We report that there was a discrepancy between *FGFR1* amplification level and FGFR1 protein expression in a number of these cell lines, and the cancers with unexpectedly low FGFR1 expression were uniformly resistant to the different FGFR inhibitors. Further

interrogation of the receptor tyrosine kinase activity in these discordant cell lines revealed co-activation of HER2 and PDGFRα caused by gene amplification or ligand overexpression maintained PI3K and MEK/ERK signaling even in the presence of FGFR inhibitor. Accordingly, co-inhibition of FGFR1 and HER2 or PDGFRα led to enhanced drug responses. In contrast, *FGFR1*-amplified high FGFR1 protein expressing lung cancers are sensitive to FGFR inhibitor monotherapy by downregulating ERK signaling. Addition of a PI3K inhibitor to these high FGFR1 protein expressing cancers further sensitized them to FGFR inhibitor. These data reveal that biomarker-directed trials for *FGFR1*-amplified SCC require assessment of FGFR1 protein expression and uncover novel therapeutic strategies for *FGFR1*-amplified SCC with low FGFR1 protein expression.

Keywords: FGFR1, lung cancer, gene amplification, biomarker

Introduction

Lung cancer is the leading cause of cancer-related death in the world. Histologically, lung cancer can be grouped as small cell-lung cancer and non-small cell lung cancer (NSCLC). NSCLC consists of adenocarcinoma, squamous cell carcinoma (SCC), and large cell carcinoma. Traditionally, NSCLC has been treated with platinum-based doublet chemotherapeutic agents, however, the identification of driver oncogenes in many of these cancers have changed the way adenocarcinomas are treated. Currently, molecularly targeted therapies targeting somatically activated oncogenes such as mutant *EGFR* or translocated *ALK*, *RET*, or *ROS1* are part of clinical treatment plans [1-3]. In contrast to the significant advances in the treatment for adenocarcinoma, there have been no targeted therapies implemented for SCC [4].

The fibroblast growth factor receptor (FGFR) signaling plays crucial roles in regulating tumor cell proliferation, angiogenesis, migration, and survival [5-7]. Deregulation of FGFR signaling has been reported due to genetic modification or overexpression of receptors in many types of cancers such as breast and bladder [6]. In lung cancer, *FGFR1* gene amplification is found in 10 to 20% of SCC samples and thought to be the commonest driver alteration in lung SCC [8-15]. While most of studies

evaluated *FGFR1* copy number by FISH analysis, the frequency defined by next generation sequencing were 7 and 9%, which were lower than FISH analysis [16, 17]. Accordingly, a few clinical trials targeting patients with histologically/cytologically confirmed advanced solid tumors with *FGFR1* or *FGFR2* amplification or *FGFR3* mutation are underway. In a phase I study, 21 patients with *FGFR1*-amplified lung SCC were treated with the pan-FGFR inhibitor NVP-BGJ398 at the maximum tolerated dose. Tumors from four of these patients achieved partial regression [18]. Another pan-FGFR inhibitor, AZD4547, achieved one partial response among 14 patients with *FGFR1* amplified stage IV lung SCC, but failed to meet the primary efficacy endpoint for continuation [19]. These initial clinical results suggest some *FGFR1*-amplified lung SCC are sensitive to FGFR inhibitors, however, the response rate is lower compared to other molecularly targeted drugs. Therefore, there is a clear need to better define the patient population that would benefit from FGFR inhibitors.

Consistent with the low rate of response in the clinic, we report four of six *FGFR1*-amplified lung cancer cells are insensitive to FGFR inhibitors. While these cell lines were all confirmed to harbor *FGFR1* gene amplification, we surprisingly found the

expression levels of mRNA and protein were widely variable. Furthermore, the lung cancers with high FGFR1 protein were sensitive to FGFR inhibitors, however, the *FGFR1* amplified lung cancers with low FGFR1 protein invariably had a co-active receptor tyrosine kinase (RTK) rendering these cancers insensitive to FGFR inhibitors. We found co-inhibition of FGFR1 and the active RTK is required to downregulate downstream signaling and achieve growth suppression. These results suggest FGFR inhibitors can be effective as monotherapy in *FGFR1*-amplified lung cancers with high FGFR1 expression; however, assaying for FGFR1 protein expression in *FGFR1*-amplified cancers is essential. In the low FGFR1 protein expressing lung cancers, there exists co-driver RTKs, in which targeting with FGFR1-based combination therapies is a sensible and effective therapeutic approach.

Results

Lung cancer cells harboring FGFR1 amplification shows variable sensitivity to FGFR1 inhibitors.

Amplification of oncogenic RTKs often predicts sensitivity to the corresponding RTK inhibitor; for instance, *HER2* amplification as determined by FISH predicts sensitivity to HER2 inhibitors in breast cancer [20]. We therefore sought to determine whether *FGFR1*-amplified lung cancer cells predicted sensitivity to FGFR inhibitor. First, we have chosen seven cell lines based on previous reports that they possessed *FGFR1* amplification [8, 9]. Characteristics of each cell line are shown in Supplementary Table 1. Results of gene copy number analysis by quantitative PCR and FISH are shown in Figure 1a, 1b, Supplementary Figure S1, and Supplementary Table 2. We excluded NCI-H2444 cells for further analysis because the cells showed extra copies of *FGFR1* as a result of polysomy of chromosome 8 (Supplementary Figure S1). Next, we determined the sensitivity of *FGFR1* amplified lung cancer cell lines (NCI-H1581, DMS-114, NCI-H520, NCI-H1703, HCC95, and Calu-3) to three FGFR inhibitors: NVP-BGJ398, PD-173074, and AZD4547. As shown in Figure 1c,

only two of these cell lines, NCI-H1581 and DMS-114, were found to be sensitive to NVP-BGJ398. We found the data to be consistent for PD-173074 and AZD4547 as well (Figure 1d and 1e). While NCI-H520 cells showed intermediate sensitivity to the FGFR inhibitors, the NCI-H1703, HCC95, and Calu-3 cells were insensitive. These results show that *FGFR1* amplification status alone is not correlated with sensitivity to FGFR1 inhibitors.

Protein expression of FGFR1 is not predicted simply by gene copy number.

We next determined whether the *FGFR1* gene is translated and transcribed in these cells. Interestingly, FGFR1 mRNA and protein expression were not always upregulated in the presence of gene amplification (Figure 1f and 1g). Therefore, no relationship was observed between protein expression and gene copy number defined by FISH (Supplementary Figure S2a) or quantitative PCR (Supplementary Figure S2b). In contrast, mRNA and protein expression was well correlated except for in the NCI-H1703 cell line (Supplementary Figure S2c). Importantly, none of the *FGFR1*-amplified, but low FGFR1 protein expressing cell lines, were sensitive to FGFR inhibitors among NCI-H1703, HCC95, and Calu-3 (Figure 1g and Supplementary

Figure S2d). We determined CpG island methylation in the *FGFR1* promoter, and found there was an absence of methylation in the HCC95 and Calu-3 cells (Supplementary Figure S3).

Both protein expression and gene amplification of FGFR1 are required to show sensitivity to FGFR inhibitor.

To determine whether high FGFR1 mRNA expression is sufficient enough to predict sensitivity to FGFR inhibitors, we evaluated the effect of PD-173074 on cell proliferation in a large panel of lung cancer cell lines (Figure 2a). Among cell lines with higher expression of FGFR1, two of 5 *FGFR1* amplified cells were sensitive to PD-173074, whereas none of the 38 cell lines without *FGFR1* amplification showed sensitivity to the FGFR inhibitor ($p < 0.05$ by fisher's exact test) (Figure 2b). Furthermore, the two cell lines that were sensitive not only had high FGFR1 mRNA expression, but had high FGFR1 protein expression. These results indicate that mRNA expression is not the sole factor to predict sensitivity and suggest that only *FGFR1*-amplified lung cancers with expected high corresponding FGFR1 protein expression are sensitive to FGFR inhibitors. In agreement with this, the Colo-699N

non-*FGFR1*-amplified cells are insensitive to NVP-BGJ398 even though the cells express comparable level of FGFR1 protein to NCI-H1581 cells (Figure 2c and 2d and Supplementary Figure S4). To further determine the efficacy of FGFR inhibitor *in vivo*, NCI-H1581 and Colo-699N were xenografted and treated with NVP-BGJ398. The data demonstrate, consistent with the *in vitro* data, *in vivo* sensitivity of xenografted NCI-H1581 tumors to NVP-BGJ398 (Figure 2e). In contrast, NVP-BGJ398 had no effect on the growth of Colo-699N tumors (Figure 2f). These data demonstrate that both amplification of *FGFR1* and high protein expression in a tumor are necessary for sensitivity to FGFR inhibitors.

FGFR inhibitor suppresses MEK/ERK signaling in FGFR-inhibitor sensitive cell lines.

We next investigated downstream signaling regulated by FGFR1 in *FGFR1*-amplified lung cancer cell lines. Since suppression of both the PI3K/AKT and MEK/ERK signaling underlies many of the antitumor effects induced by TKIs in RTK-addicted tumors, which converge on the mTORC1 pathway [21, 22], these signaling pathways were investigated. We found the *FGFR1*-amplified lung cancer cell lines

had variable levels of FGFR1 phosphorylation and protein levels (Figure 3a). Interestingly, FGFR inhibitor treatment downregulated phosphorylation of ERK as well as S6, a readout for mTORC1 activity [23], in FGFR inhibitor-sensitive and intermediately sensitive cell lines. However, the drug has no effect on ERK and S6 phosphorylation in resistant cells (Figure 3b). Of note, AKT phosphorylation was not affected by FGFR inhibitor in either the sensitive or resistant group. Reduction of FGFR1 mRNA and protein by transfection of FGFR1-specific short-interfering siRNA recapitulated the inhibition of pERK following FGFR inhibitor (Figure 3c). These results demonstrate that FGFR1 mainly regulates MAPK signaling in FGFR inhibitor sensitive cell lines. Consistent with this, the extent of ERK suppression is associated with the degree of growth inhibition induced by FGFR inhibitor. NVP-BGJ398 suppressed ERK phosphorylation in a dose-dependent manner that is associated with growth suppression induced by the drug (Figure 3d to 3f). Interestingly, the most sensitive cell line, NCI-H1581, has no measurable AKT phosphorylation (Figure 3a), raising the possibility that PI3 kinase inhibition may further sensitize the *FGFR1*-amplified and high FGFR1 protein DMS-114 and NCI-H520 cell lines. Indeed, the combination of a PI3 kinase inhibitor GDC-0941 and NVP-BGJ398 led to complete suppression of S6 phosphorylation (Figure 3g) and

enhanced growth suppression compared to either drug alone (Figure 3h). These data indicate that in *FGFR1-* amplified lung cancer cell lines with high FGFR1 protein expression, FGFR inhibitors block pERK and TORC1 signaling, and the addition of a PI3K inhibitor further sensitizes these cancers through greater suppression of the PI3K/TORC1 pathway. However, in *FGFR1*-amplified lung cancer cells with low FGFR1 expression, pERK and TORC signaling are unaffected by FGFR inhibition.

Additional driver oncogene activation mitigates the effect of FGFR1 inhibition in low FGFR1 protein expressing cells.

To elucidate the mechanism of primary resistance to FGFR inhibitors in *FGFR1* amplified lung cancers, phosphorylation status of RTKs were examined in the insensitive cell lines. In the NCI-H1703 cell line, we identified high PDGFRα phosphorylation, consistent with reported amplification of *PDGFRa* in this cell line [24, 25] (Figure 4a). In the Calu-3 cell line, we identified high phosphorylation of EGFR family proteins and MET on activation loop residues (Figure 4b). This cell line has reported *HER2* amplification [26]. In the HCC95 cell lines, an RTK array showed a similar pattern of EGFR family protein activation as the Calu-3 cell line (Figure 5a).

However, the cells did not have an *EGFR* mutation (Supplementary Table 1) or *HER2* amplification (Figure 5b). Activation of EGFR family receptors can occur via ligand binding, resulting in hetero- and homo-dimerization with other EGFR family proteins. Recent findings showed that overexpression of neuregulin-1 (NRG1) can also drive HER3 activation by an autocrine signaling loop in a subset of non-*HER2* amplified cancers [27]. Indeed, we found that HCC95 cells express high amounts of NRG1 mRNA and protein compared to other *FGFR1*-amplified cells (Figure 5c and d). Consistently, knockdown of NRG1 inhibited cell viability in HCC95 cells, while it had no effect on NCI-H520 cells (Figure 5e and 5f). Furthermore, addition of serum free media conditioned from the HCC95 cells activated HER3 protein and downstream AKT signaling in NCI-H1581 cells expressing low NRG1 (Figure 5g). These results demonstrate that autocrine production of NRG1 maintains the survival of HCC95 cells following FGFR inhibitor treatment.

We next sought to determine whether addition of the appropriate TKI sensitized the NCI-H1703, HCC95 and Calu-3 cell line to FGFR inhibitor. Importantly, the addition of NVP-BGJ398 to an inhibitor targeting the co-activated RTK enhanced inhibition of cell growth in each *FGFR1*-amplified lung cancer with low FGFR1 protein

expression in five day growth assays (Figure 6a). Furthermore, combination of the FGFR inhibitor with the RTK inhibitor achieved better suppression of S6 phosphorylation and expression of the mTORC1-sensitive anti-apoptotic protein MCL-1 [28], resulting in enhanced apoptosis induction in these cells (Figure 6b). Intriguingly, phosphorylation of the FRS2, adaptor protein which mediate signaling from FGFR1 to effector proteins was not suppressed by either FGFR inhibitor or the single-agent RTK inhibitor, but was achieved by the combination of the drugs. These data implicate the interaction of FGFR1 and HER2 in the HCC95 and Calu-3 cells, and PDGFRα in the H1703 cells. Collectively, these data demonstrate that co-activation of other RTKs mitigates the effect of FGFR inhibitor in *FGFR1* amplified lung cancer with low FGFR1 protein expression. Consequentially, the combination of FGFR inhibitors with either Lapatinib or Imatinib is effective.

Existence of co-activated RTKs in low FGFR1 expression in patients with FGFR1 amplified lung SCC

To further expand our findings, we have investigated FGFR1 protein expression in 25 patient with *FGFR1* gene amplified lung SCC identified by FISH analysis (Figure

7a). IHC stain identified only six of 25 tumors were positive for FGFR1 protein expression; only one case exhibited diffuse and strong expression. Furthermore, FGFR1 was not expressed in two cases harboring both *FGFR1* and *PDGFRa* gene amplification. To validate the discrepancy between protein expression and gene amplification of *FGFR1* using an independent data set, we analyzed an RNA SEQ data set of 178 lung SCCs from The Cancer Genome Atlas (TCGA) project. The analysis revealed that only eight samples show *FGFR1* amplification with concomitant high mRNA expression among 30 *FGFR1*-amplified cancers (Figure 7b). Interestingly, overexpression of NRG1 is mutually exclusive to *HER2* and *PDGFRa* amplification among *FGFR1*-amplified cancers (Figure 7b). Furthermore, tumors with gene amplification and mRNA expression do not have any co-existing driver oncogenes (Figure 7b). Collectively, these data are consistent with our findings in this study that *FGFR1* amplified lung cancers with low FGFR1 protein depend on other RTKs for their growth, while *FGFR1*-amplified cancers with high FGFR1 protein expression rely solely on FGFR1.

Discussion

We have demonstrated that only some *FGFR1* amplified lung cancer cell lines are sensitive to FGFR inhibitors. We further demonstrate that the cases which have amplified *FGFR1* and insensitive have discordant levels of protein. These cancers with unexpectedly low levels of FGFR1 protein do not have MEK/ERK signaling under the control of FGFR1; instead, other co-active RTKs co-regulate this pathway. Therefore, FGFR inhibitors show efficacy only in the subset of *FGFR1*-amplified lung cancers that have high protein expression and activate the MEK/ERK pathway.

The relationship between gene copy number and protein expression in *FGFR1*-amplified cancers has been studied using tumor samples [12, 13, 15, 29]. Kohler and colleagues studied copy number and protein expression levels of FGFR1 in 133 lung SCCs using FISH and IHC [12]. While increased FGFR1 protein expression levels correlated with gene copy number as a whole, they also pointed out discordant cases exist in their cohort. Similarly, Kim et al. analyzed 262 patients with lung SCC and showed association between *FGFR1* gene amplification and mRNA expression, however, about half of the cases expressed less than 1.5 fold of FGFR1 mRNA

compared to the housekeeping gene [13]. Intriguingly, a patient derived tumor xenograft harboring *FGFR1* amplification but discordant, low-level protein was less sensitive to AZD4547 compared to four other models harboring *FGFR1* amplification with consistently high-level FGFR1 protein expression [30]. Loss of FGFR1 protein expression in the presence of gene amplification could be mediated by aberrant DNA promoter methylation, a common feature of many human cancers [31, 32] . Whereas a large CpG island is observed in the promoter region of FGFR1 gene defined by UCSC genome browser, no methylation was observed in HCC95 and Calu-3 cells (Supplementary Figure S3). Other mechanisms including aberrant expression of microRNAs need to be considered in future studies. These results support the idea that both gene amplification and protein expression are needed for patient selection. The importance of FGFR1 protein expression in FGFR inhibitor sensitivity was also shown in a recent study by Wynes et al [29]; However, they proposed that FGFR1 mRNA and protein expression are the predictors of FGFR inhibitor Ponatinib regardless of gene amplification across all lung cancer histologies. In adenocarcinoma, some cells express FGFR1 protein without gene amplification, however, drug screening with the FGFR inhibitor PD-173074 indicates that none of the 51 lung adenocarcinoma cell lines tested were sensitive to PD-173074 (Figure 2a

and 2b). Furthermore, only NCI-H1581 and DMS-114 cells are sensitive to PD-173074 and NVP-BGJ398 among 14 cell lines identified to be sensitive to Ponatinib in the study (Supplementary Table 3). These results suggest *FGFR1*-gene amplification is important to predict sensitivity against FGFR inhibitors, and the apparent discrepancy may be a result of drug promiscuity; in contrast to NVP-BGJ398 and AZD4547 which are relatively selective pan-FGFR inhibitors [33, 34], Ponatinib inhibits a number of non-FGFR kinases with IC_{50} concentrations less than 10nM, including VEGFR, PDGFR, EPH receptors, SRC, KIT, and RET [35].

In this study, we found that *FGFR1*-amplified lung cancer cells that showed resistance to FGFR inhibitors had additional RTKs that activated survival signaling. We demonstrated Calu-3 *HER2*-amplified and NCI-H1703 *PDGFRα*-amplified cells are insensitive to NVP-BGJ398 and co-inhibition of HER2 and PDGFRα, respectively, lead to potent growth suppression. In addition, we found the HCC95 cell line possessed overexpression of NRG1, leading to activation of HER3. Co-inhibition with lapatinib sensitized these cells to FGFR inhibitor. Previous studies have also shown cross talk between FGFR and ERBB pathway in multiple tumor types [36-38]. In lung cancer, activation of FGFR pathway is a cause of acquired resistance to EGFR

inhibitors in *EGFR* mutant cancer cell lines [36]. Also, a switch from dependency on FGFR3 to ERBB family members were observed in FGFR inhibitor resistant FGFR3 amplified or translocated lung cancers [38]. Interestingly, we have demonstrated that tumors harboring both *FGFR1* and *PDGFRa* amplification did not express FGFR1 protein in our tissue microarray analysis. Furthermore, analysis of 178 lung SCC tumors from TCGA identified overexpression of NRG1 as mutually exclusive to *HER2* and *PDGFRa* amplification. Notably, none of these alterations were identified in high mRNA expressing *FGFR1* amplified tumors, consistent with our *in vitro* findings. Importantly, tumors with *FGFR1* gene amplification that have concomitant high FGFR1 mRNA expression or positive FGFR1 IHC staining consist of only a subset of *FGFR1* amplified tumors. These data are consistent with our in vitro findings, raising the possibility that stratification by combining FISH with protein expression analysis, such as immunohistochemistry, would inform which patients would be expected to respond. Furthermore, a search for other co-driver RTKs through sequencing and *HER2* FISH analysis may identify patients whom would respond to FGFR-based combination therapies.

While *HER2* amplification is defined as an HER2/chromosome 17 centromere ratio

of more than 2.2, which correlates well with the response to anti-HER2 antibody in breast and gastric cancer, the definition of *FGFR1* amplification has not been established yet [10, 11, 13, 14, 30, 39, 40]. We observed no association between amplification level of *FGFR1* and sensitivity to FGFR inhibitors in our cell line panel. In a phase I trial of AZD4547, although patients with FGFR1:CEP8 ratios of more than 2.8 appeared to have better growth suppression in comparison to patients with FGFR1:CEP8 ratios between 2 to 2.8, the difference was not statistically significant and only one of seven patients with high *FGFR1* amplified tumor achieved a partial response [19]. The FGFR1 locus is heterogeneous, therefore the limitation of the resolution of FISH analysis may lead to false-positive detection of FGFR1 amplification and might result in the lack of association with efficacy to FGFR inhibitor [4, 41]. We also observed that gene copy number analysis by quantitative PCR did not correlate with FISH results because of aneuploidy. As *FGFR1* copy number is determined by quantitative PCR and used as a selection criterion in current NVP-BGJ398 studies [18], the usefulness of gene copy number analysis and the relationship between response and copy number needs to be clarified.

Activation of FGFR1 signaling can lead to tumorigenesis by affecting a number of

downstream signaling. While signal transduction pathways initiating FGFR-dependent oncogenesis differ depending on cellular context [42], our results demonstrated that the MAPK/ERK pathway is the major downstream pathway under control of FGFR1 in *FGFR1*-amplified lung cancer cell lines. In *FGFR1*-amplified but low FGFR1 protein expressing lung cancers, other RTK's have significant control of MEK/ERK signaling; co-inhibition with FGFR inhibitors, however, are required for marked suppression. This demonstrates that *FGFR1*-amplified lung cancers with low FGFR1 protein expression require an additional, aberrantly active RTK to activate the MEK/ERK pathway, the co-existence of which may be necessary for transformation. Furthermore, requirement of co-inhibition to suppress FRS2 phosphorylation may suggest a crosstalk between FGFR1 and the co-active RTK.

Lastly, the addition of a PI3K inhibitor enhanced efficacy of FGFR inhibitor in the DMS-114 and NCI-H520 cell lines. In these *FGFR1*-amplified lung cancers with high FGFR1 protein and intermediate to high sensitivity to FGFR inhibitors, treatment with FGFR inhibitor led to downregulated MEK/ERK signaling but did not affect PI3K/AKT signaling. Effective treatments with TKIs in oncogene-addicted cancers

invariably lead to decreased signaling along the downstream PI3K/AKT and MEK/ERK pathways. Interestingly, the FGFR inhibitor PD173074 downregulates both AKT and ERK signaling in multiple *FGFR2*-amplified gastric cancer cell lines, resulting in cell death [43]. Therefore, downstream signaling regulated by amplified *FGFR* may depend on which family member protein is altered.

In conclusion, we have demonstrated that high FGFR1 protein expression is surprisingly absent in a significant number of *FGFR1*-amplified lung cancers, and these cancers are uniformly resistant to FGFR inhibitors. As such, the identification of co-existing driver RTKs are necessary to treat patients with *FGFR1*-amplified tumors with low protein expression. Notably, a master protocol study, Lung-MAP project is designed to screen samples by next-generation sequencing and planned to enroll patients in biomarker-driven phase II/III studies in SCC lung carcinoma [44]. Here, we propose an alternative screening strategy for *FGFR1*-amplified lung SCCs (Figure 7c), which could ultimately help stratify patients to the most effective therapy.

Materials and Methods

Cell lines and reagents

The lung cancer cell lines NCI-H1581, DMS-114, NCI-H520, NCI-H1703, Calu-3, and NCI-H2444 were purchased from the American Type Culture Collection (ATCC, Manassas, VA, USA). HCC95 was obtained from the Korean Cell Line Research Foundation. MRC-5 was obtained from the Japanese Cell Research Bank. Colo-699N was obtained from the European Collection of Cell Cultures. Cells were cultured in RPMI1640 (Invitrogen, Carlsbad, CA, USA) with 5% FBS. All cell lines were tested and authenticated by short tandem repeat (STR) analysis with GenePrint 10 System (Promega, Milan, Italy) by the Japanese Cell Research Bank. Cells were regularly screened for Mycoplasma using a MycoAlert Mycoplasma Detection Kit (Lonza, Verviers, Belgium). NVP-BGJ398, AZD4547, PD173074, and imatinib were obtained from Active Biochem (Hong Kong, China). Lapatinib was purchased from Selleck (Houston, TX, USA). Compounds were dissolved in DMSO to a final concentration of 10 mmol/l and stored at –20°C.

Growth assay

Assay was performed as previously described [45]. Luminescence was recorded by

iMark Microplate Reader (Bio-Rad, Hercules, CA, USA).

Gene copy number analysis

Genomic DNA was extracted by DNeasy Blood & Tissue Kit (QIAGEN, Velno, Limburg, Netherlands). Gene copy number of *FGFR1* was analyzed using TaqMan gene copy number assay (Assay ID: Hs01694937_cn, Applied Biosystems, Carlsbad, CA, USA), according to the manufacturer's instructions. TaqMan Copy Number Reference Assay, human RNase P was used as the endogenous reference gene. Fold increase in copy number was calculated as the ratio of the FGFR1 signal in each cell lines to that obtained in the normal *FGFR1* gene expressing MRC-5 cells.

Quantitative PCR analysis

RNA was extracted using the RNeasy kit (QIAGEN), and cDNA was generated by the Omniscript Reverse Transcriptase kit (QIAGEN) according to the manufacturer's instructions. The amount of amplicon was determined with the Mx3005P qPCR System using TaqMan Universal PCR Master Mix (Applied Biosystems). Each sample was normalized to the housekeeping gene actin. All samples were analyzed in triplicate, and the relative expression to MRC-5 was

determined. Primer sets are FGFR1 forward (5'-TAATGGACTCTGTGGTGCCCTC-3') and FGFR1 reverse (5'-ATGTGTGGTTGATGCTGCCG-3'); ß-actin forward (5'-TACATGGCTGGGGTGTTGAA-3') and ß-actin reverse (5'-AAGAGAGGCATCCTCACCCT-3').

Protein analysis

For Western blot analysis, lysates were prepared using Cell Lysis Buffer (Cell Signaling Technologies, Danvers, MA, USA); the procedure for Western blotting was as previously described [45]. Antibodies used in this study are summarized in Supplementary Table 4. Human phospho-RTK arrays were obtained from R&D Systems (Minneapolis, MN, USA) and used according to the manufacturer's instructions. The method to detect secreted NRG1 was previously described [27]. All immunoblots are representative of three independent experiments and RTK array was replicated twice.

siRNA knockdown

Cells were seeded into 6-well plates at a density of 1-2 × 10^5 cells/well. Twenty-four hours later, cells were transfected with two siRNAs against FGFR1 (Dharmacon,

Lafayette, CO, USA) or Stealth RNAi-negative control low GC Duplex #3 (Invitrogen) using Lipofectamine RNAiMAX (Invitrogen). Transfected cells were cultured at 37°C for 5 days before analysis.

Lentiviral shRNA experiments

shNRG1 constructs were obtained from Openbiosystems (Carlsbad, CA, USA) and control shRNA was from Addgene (Cambridge, MA, USA). The target sequences of NRG1 were CGTGGAATCAAACGAGATCAT for shNRG #1 and GCCTCAACTGAAGGAGCATAT for shNRG1 #2, respectively. Preparation of lentivirus and infections were performed as previously described [45].

Fluorescence in situ hybridization (FISH)

Bacterial artificial chromosome (BACPAC Resources, Oakland CA, USA) of RP11-148D21 specific to the *FGFR1* locus (8p11.23-11.22) was labeled with SpectrumOrange™ using a nick translation kit (Abbott, Abbott Park IL, USA). Centromere 8 labeled with SpectrumGreen™ (CEP8TM, Abbott) was paired for copy number control. FISH was performed using standard methods and included a RNase A treatment [46]. Only nuclei with unambiguous CEP8TM signals were scored for the

FGFR1 signal number. Two independent researchers (HK and KK) blindly scored thirty cells each to determine the gene copy number and the pattern of gene amplification. The results were concordant between two researchers in all cell lines. *FGFR1* copy number relative to the chromosome 8 centromere copy number was calculated as the average of 60 cells. Gene amplification was defined as cells harboring FGFR1 copy number control ratio 2.0 or higher. The PathVysion HER-2 DNA Probe Kit (PathVysion Kit, Abbott) was used to determine amplification of the HER-2/neu gene and assessed by LSI Medience Corporation Japan. Images were captured using a standard setting by Axio Imager 72 (Zeiss, Thornwood, NY, USA).

Xenograft mouse studies

For xenograft experiments, a suspension of 5×10^6 cells was injected subcutaneously into the flanks of 6- to 8-week-old male nude mice (Clea, Tokyo, Japan). The care and treatment of experimental animals were in accordance with institutional guidelines. The sample size was 12. Mice were randomized (n = 6 per group) once the mean tumor volume reached approximately 200 mm^3, and there were no exclusion criteria. All data were analysed unblinded and verified by two independent researchers (HK and HE). NVP-BGJ398 was dissolved in acetic acid/acetate buffer pH 4.6/PEG300

1:1. Tumors were measured twice weekly using calipers, and volume was calculated using the following formula: length × width^2 × 0.52. Mice were monitored daily for body weight and general condition. Xenograft experiments were approved by the ethical committee on the Institute for Experimental Animals, Kanazawa University Advanced Science Research Center.

Immunohistochemistry (IHC)

Immunohistochemistry was performed on TMA sections using rabbit polyclonal antibody to FGFR1 (abcam, Cambridge, MA, USA, ab137781, 1:50). Staining was performed using the Leica RX Bond Autostainer (Leica Biosystems, IL, USA). Antigen retrieval was performed in ER 1 (Citrate buffer) for 20 min and stained using the Bond Polymer Refine Protocol under the IHC Modified F Protocol as previously described [47]. Positive control included xenografted tumor samples of NCI-H1581. Each TMA tumor core was assessed by a pathologist (MMK) semi-quantitatively based on the extent of tumor cells with membranous staining and the intensity of membranous staining as follows: 0, no staining; 1+, any staining in <50% of tumor cells or only faint/weak staining in ≥50% of tumor cells; 2+, moderate/strong staining in ≥50% of tumor cells. Multiples cores from each patient were collectively

assessed. Cases with 1+ and 2+ staining were regarded as positive. FISH analysis of *FGFR1* and *PDGFRa* in these samples was previously described [10]. This study was approved by The Institutional Review Board at Massachusetts General Hospital. Informed consent was obtained from all patients.

Analysis of publicly available dataset

Information regarding *FGFR1*, *HER2*, and *PDGFRa* amplification and FGFR1 and NRG1 expression data of primary lung SCCs were from The Cancer Genome Atlas (TCGA) repository and obtained through the cBioPortal [16, 48, 49]. FGFR1 and NRG1 expression was defined as positive when the Z-score of mRNA level was higher than 2.

Statistical analysis

Statistical tests were performed by linear regression analysis and Fisher's exact test as indicated. Differences were considered statistically different if $P<0.05$.

Conflict of interest

The authors declare no conflict of interest.

Acknowledgements

We wish to thank Dr. Shuta Tomida at Okayama University for his assistance with the statistics. This work is supported by Grants-in-Aid for Scientific Research (H. Ebi, 26830105; S. Yano, 21390256), Scientific Research on Innovative Areas "Integrative Research on Cancer Microenvironment Network" (S. Yano, 22112010A01), and Grant-in-Aid for Project for Development of Innovative Research on Cancer Therapeutics (P-Direct) from the Ministry of Education, Culture, Sports, Science, and Technology (MEXT) of Japan.

Supplementary Information accompanies this paper on the Oncogene website (http://www.nature.com/onc)

References

1 Lynch TJ, Bell DW, Sordella R, Gurubhagavatula S, Okimoto RA, Brannigan BW *et al*. Activating mutations in the epidermal growth factor receptor underlying responsiveness of non-small-cell lung cancer to gefitinib. *N Engl J Med* 2004; 350: 2129-2139.

2 Soda M, Choi YL, Enomoto M, Takada S, Yamashita Y, Ishikawa S *et al*. Identification of the transforming EML4-ALK fusion gene in non-small-cell lung cancer. *Nature* 2007; 448: 561-566.

3 Meador CB, Micheel CM, Levy MA, Lovly CM, Horn L, Warner JL *et al*. Beyond histology: translating tumor genotypes into clinically effective targeted therapies. *Clin Cancer Res* 2014; 20: 2264-2275.

4 Gandara DR, Hammerman PS, Sos ML, Lara PN, Jr., Hirsch FR. Squamous cell lung cancer: from tumor genomics to cancer therapeutics. *Clin Cancer Res* 2015; 21: 2236-2243.

5 Dieci MV, Arnedos M, Andre F, Soria JC. Fibroblast growth factor receptor inhibitors as a cancer treatment: from a biologic rationale to medical perspectives. *Cancer Discov* 2013; 3: 264-279.

6 Brooks AN, Kilgour E, Smith PD. Molecular pathways: fibroblast growth factor signaling: a new therapeutic opportunity in cancer. *Clin Cancer Res* 2012; 18: 1855-1862.

7 Dienstmann R, Rodon J, Prat A, Perez-Garcia J, Adamo B, Felip E *et al.* Genomic aberrations in the FGFR pathway: opportunities for targeted therapies in solid tumors. *Ann Oncol* 2014; 25: 552-563.

8 Weiss J, Sos ML, Seidel D, Peifer M, Zander T, Heuckmann JM *et al.* Frequent and focal FGFR1 amplification associates with therapeutically tractable FGFR1 dependency in squamous cell lung cancer. *Sci Transl Med* 2010; 2: 62ra93.

9 Dutt A, Ramos AH, Hammerman PS, Mermel C, Cho J, Sharifnia T *et al.* Inhibitor-sensitive FGFR1 amplification in human non-small cell lung cancer. *PLoS One* 2011; 6: e20351.

10 Heist RS, Mino-Kenudson M, Sequist LV, Tammireddy S, Morrissey L, Christiani DC *et al.* FGFR1 amplification in squamous cell carcinoma of the lung. *J Thorac Oncol* 2012; 7: 1775-1780.

11 Schildhaus HU, Heukamp LC, Merkelbach-Bruse S, Riesner K, Schmitz K, Binot E *et al.* Definition of a fluorescence in-situ hybridization score identifies high- and low-level FGFR1 amplification types in squamous cell lung cancer. *Mod Pathol* 2012; 25: 1473-1480.

12 Kohler LH, Mireskandari M, Knosel T, Altendorf-Hofmann A, Kunze A, Schmidt A *et al.* FGFR1 expression and gene copy numbers in human lung cancer. *Virchows Arch* 2012; 461: 49-57.

13 Kim HR, Kim DJ, Kang DR, Lee JG, Lim SM, Lee CY *et al.* Fibroblast growth

factor receptor 1 gene amplification is associated with poor survival and cigarette smoking dosage in patients with resected squamous cell lung cancer. *J Clin Oncol* 2013; 31: 731-737.

14 Tran TN, Selinger CI, Kohonen-Corish MR, McCaughan BC, Kennedy CW, O'Toole SA *et al.* Fibroblast growth factor receptor 1 (FGFR1) copy number is an independent prognostic factor in non-small cell lung cancer. *Lung Cancer* 2013; 81: 462-467.

15 Seo AN, Jin Y, Lee HJ, Sun PL, Kim H, Jheon S *et al.* FGFR1 amplification is associated with poor prognosis and smoking in non-small-cell lung cancer. *Virchows Arch* 2014; 465: 547-558.

16 Cancer Genome Atlas Research N. Comprehensive genomic characterization of squamous cell lung cancers. *Nature* 2012; 489: 519-525.

17 Helsten T, Elkin S, Arthur E, Tomson BN, Carter J, Kurzrock R. The Fgfr Landscape in Cancer: Analysis of 4853 Tumors by Next Generation

Sequencing. *Clin Cancer Res* 2015.

18 Nogova L, Sequist LV, Cassier PA, Hidalgo M, Delord JP, Schuler MH *et al.* Targeting FGFR1-amplified lung squamous cell carcinoma with the selective pan-FGFR inhibitor BGJ398. *J Clin Oncol* 2014; 32: (suppl; abstr 8034).

19 Paik PK, Shen R, Ferry D, Soria JC, Mathewson A, Kilgour E *et al.* A phase 1b open-label multicenter study of AZD4547 in patients with advanced squamous cell lung cancers: Preliminary antitumor activity and pharmacodynamic data. *J Clin Oncol* 2014; 32: (suppl; abstr 8035).

20 Slamon DJ, Leyland-Jones B, Shak S, Fuchs H, Paton V, Bajamonde A *et al.* Use of chemotherapy plus a monoclonal antibody against HER2 for metastatic breast cancer that overexpresses HER2. *N Engl J Med* 2001; 344: 783-792.

21 Engelman JA, Janne PA. Mechanisms of acquired resistance to epidermal growth factor receptor tyrosine kinase inhibitors in non-small cell lung cancer.

Clin Cancer Res 2008; 14: 2895-2899.

22 Faber AC, Li D, Song Y, Liang MC, Yeap BY, Bronson RT *et al.* Differential induction of apoptosis in HER2 and EGFR addicted cancers following PI3K inhibition. *Proc Natl Acad Sci U S A* 2009; 106: 19503-19508.

23 Laplante M, Sabatini DM. mTOR signaling at a glance. *J Cell Sci* 2009; 122: 3589-3594.

24 Rikova K, Guo A, Zeng Q, Possemato A, Yu J, Haack H *et al.* Global survey of phosphotyrosine signaling identifies oncogenic kinases in lung cancer. *Cell* 2007; 131: 1190-1203.

25 McDermott U, Ames RY, Iafrate AJ, Maheswaran S, Stubbs H, Greninger P *et al.* Ligand-dependent platelet-derived growth factor receptor (PDGFR)-alpha activation sensitizes rare lung cancer and sarcoma cells to PDGFR kinase inhibitors. *Cancer Res* 2009; 69: 3937-3946.

26 Lewis Phillips GD, Li G, Dugger DL, Crocker LM, Parsons KL, Mai E *et al.* Targeting HER2-positive breast cancer with trastuzumab-DM1, an antibody-cytotoxic drug conjugate. *Cancer Res* 2008; 68: 9280-9290.

27 Wilson TR, Lee DY, Berry L, Shames DS, Settleman J. Neuregulin-1-mediated autocrine signaling underlies sensitivity to HER2 kinase inhibitors in a subset of human cancers. *Cancer Cell* 2011; 20: 158-172.

28 Hata AN, Engelman JA, Faber AC. The BCL2 Family: Key Mediators of the Apoptotic Response to Targeted Anticancer Therapeutics. *Cancer Discov* 2015; 5: 475-487.

29 Wynes MW, Hinz TK, Gao D, Martini M, Marek LA, Ware KE *et al.* FGFR1 mRNA and protein expression, not gene copy number, predict FGFR TKI sensitivity across all lung cancer histologies. *Clin Cancer Res* 2014; 20: 3299-3309.

30 Zhang J, Zhang L, Su X, Li M, Xie L, Malchers F *et al.* Translating the

therapeutic potential of AZD4547 in FGFR1-amplified non-small cell lung cancer through the use of patient-derived tumor xenograft models. *Clin Cancer Res* 2012; 18: 6658-6667.

31 Robertson KD. DNA methylation, methyltransferases, and cancer. *Oncogene* 2001; 20: 3139-3155.

32 Montenegro MF, Sanchez-del-Campo L, Fernandez-Perez MP, Saez-Ayala M, Cabezas-Herrera J, Rodriguez-Lopez JN. Targeting the epigenetic machinery of cancer cells. *Oncogene* 2015; 34: 135-143.

33 Guagnano V, Kauffmann A, Wohrle S, Stamm C, Ito M, Barys L *et al.* FGFR genetic alterations predict for sensitivity to NVP-BGJ398, a selective pan-FGFR inhibitor. *Cancer Discov* 2012; 2: 1118-1133.

34 Gavine PR, Mooney L, Kilgour E, Thomas AP, Al-Kadhimi K, Beck S *et al.* AZD4547: an orally bioavailable, potent, and selective inhibitor of the fibroblast growth factor receptor tyrosine kinase family. *Cancer Res* 2012; 72:

2045-2056.

35 O'Hare T, Shakespeare WC, Zhu X, Eide CA, Rivera VM, Wang F *et al.* AP24534, a pan-BCR-ABL inhibitor for chronic myeloid leukemia, potently inhibits the T315I mutant and overcomes mutation-based resistance. *Cancer Cell* 2009; 16: 401-412.

36 Terai H, Soejima K, Yasuda H, Nakayama S, Hamamoto J, Arai D *et al.* Activation of the FGF2-FGFR1 autocrine pathway: a novel mechanism of acquired resistance to gefitinib in NSCLC. *Mol Cancer Res* 2013; 11: 759-767.

37 Harbinski F, Craig VJ, Sanghavi S, Jeffery D, Liu L, Sheppard KA *et al.* Rescue screens with secreted proteins reveal compensatory potential of receptor tyrosine kinases in driving cancer growth. *Cancer Discov* 2012; 2: 948-959.

38 Wang J, Mikse O, Liao RG, Li Y, Tan L, Janne PA *et al.* Ligand-associated ERBB2/3 activation confers acquired resistance to FGFR inhibition in

FGFR3-dependent cancer cells. *Oncogene* 2015; 34: 2167-2177.

39 Wolff AC, Hammond ME, Hicks DG, Dowsett M, McShane LM, Allison KH *et al.* Recommendations for human epidermal growth factor receptor 2 testing in breast cancer: American Society of Clinical Oncology/College of American Pathologists clinical practice guideline update. *J Clin Oncol* 2013; 31: 3997-4013.

40 Pros E, Lantuejoul S, Sanchez-Verde L, Castillo SD, Bonastre E, Suarez-Gauthier A *et al.* Determining the profiles and parameters for gene amplification testing of growth factor receptors in lung cancer. *Int J Cancer* 2013; 133: 898-907.

41 Malchers F, Dietlein F, Schottle J, Lu X, Nogova L, Albus K *et al.* Cell-autonomous and non-cell-autonomous mechanisms of transformation by amplified FGFR1 in lung cancer. *Cancer Discov* 2014; 4: 246-257.

42 Turner N, Grose R. Fibroblast growth factor signalling: from development to

cancer. *Nat Rev Cancer* 2010; 10: 116-129.

43 Kunii K, Davis L, Gorenstein J, Hatch H, Yashiro M, Di Bacco A *et al.* FGFR2-amplified gastric cancer cell lines require FGFR2 and Erbb3 signaling for growth and survival. *Cancer Res* 2008; 68: 2340-2348.

44 Herbst RS, Gandara DR, Hirsch FR, Redman MW, LeBlanc M, Mack PC *et al.* Lung Master Protocol (Lung-MAP)-A Biomarker-Driven Protocol for Accelerating Development of Therapies for Squamous Cell Lung Cancer: SWOG S1400. *Clin Cancer Res* 2015; 21: 1514-1524.

45 Ebi H, Corcoran RB, Singh A, Chen Z, Song Y, Lifshits E *et al.* Receptor tyrosine kinases exert dominant control over PI3K signaling in human KRAS mutant colorectal cancers. *J Clin Invest* 2011; 121: 4311-4321.

46 Ooi A, Inokuchi M, Harada S, Inazawa J, Tajiri R, Kitamura SS *et al.* Gene amplification of ESR1 in breast cancers--fact or fiction? A fluorescence in situ hybridization and multiplex ligation-dependent probe amplification study. *J*

Pathol 2012; 227: 8-16.

47 Niederst MJ, Sequist LV, Poirier JT, Mermel CH, Lockerman EL, Garcia AR *et al*. RB loss in resistant EGFR mutant lung adenocarcinomas that transform to small-cell lung cancer. *Nat Commun* 2015; 6: 6377.

48 Cerami E, Gao J, Dogrusoz U, Gross BE, Sumer SO, Aksoy BA *et al*. The cBio cancer genomics portal: an open platform for exploring multidimensional cancer genomics data. *Cancer Discov* 2012; 2: 401-404.

49 Gao J, Aksoy BA, Dogrusoz U, Dresdner G, Gross B, Sumer SO *et al*. Integrative analysis of complex cancer genomics and clinical profiles using the cBioPortal. *Sci Signal* 2013; 6: pl1.

Figure legends

Figure 1. Protein expression is associated with sensitivity to FGFR inhibitor in *FGFR1* amplified lung cancer cell lines.

(a) *FGFR1* gene copy number was analyzed by Taqman gene copy number assay. Fold increase in copy number was calculated as the ratio of the FGFR1 signal in each cell lines to that of obtained in human fetal lung fibroblast MRC-5 cells. Error bars represent SD of triplicate independent experiments.

(b) Copy number of *FGFR1* measured by FISH. Centromere 8 was co-stained and the ratio of *FGFR1* to CEP8 is shown.

(c, d, e) Six *FGFR1* amplified cell lines were treated with three pan-FGFR inhibitors, NVP-BGJ398 (c), AZD4547 (d), and PD-173074 (e). Error bars represent mean ± SD.

(f) mRNA level of FGFR1 was analyzed by quantitative PCR. Fold increase in mRNA to MRC-5 cells was shown. Error bars represent SD of triplicate independent experiments.

(g) The levels of FGFR1 protein expression were shown. Immunoblots in Figure 3a were quantified relative to β-actin levels and expressed as fold levels to the MRC-

5 cells.

Figure 2. FGFR1 protein expressing, but *FGFR1* non-amplified cells are insensitive to pan-FGFR inhibitors.

(a) IC50 data to PD-173074 was obtained from The Genomics of Drug Sensitivity in Cancer Project (http://www.cancerrxgene.org/). FGFR1 mRNA expression data was obtained from Cancer Cell Line Encyclopedia (http://www.broadinstitute.org/ccle/home). Each cells were plotted by FGFR1 mRNA (x axis) and IC50 to PD-173074 (Y axis). Sensitive cells (NCI-H1581 and DMS-114) were denoted in red.

(b) Expression of FGFR1 mRNA is not enough to be sensitive to FGFR inhibitor. The relationship between gene amplification and sensitivity to FGFR inhibitor among FGFR1 mRNA expressed cells were determined by fisher's exact test. FGFR1 expression was defined as high when mRNA level was higher than median.

(c) Non-*FGFR1* amplified Colo-699N cells have comparable FGFR1 protein

expression to *FGFR1* amplified NCI-H1581 cells. Cells were lysed and blotted by indicated antibodies.

(d) NCI-H1581 and Colo-699N cells were treated with NVP-BGJ398. Error bars represent mean ± SD.

(e, f) Xenograft tumors derived from the NCI-H1581 (e) or Colo-699N (f) cells were developed. Once they achieved an average size of 200 mm^3, the tumors were treated with 25 mg/kg of NVP-BGJ398 by oral gavage once daily, and tumor volumes were plotted over time (mean ± SEM).

Figure 3. FGFR1 regulates ERK signaling in both *FGFR1* amplified and protein expressing cells.

(a) Cells were lysed and blotted with indicated antibodies. Independent experiments were performed three times, and a representative result is shown.

(b) Cells were treated with 1μM NVP-BGJ398 for 24h and cell lysates were blotted with indicated antibodies

(c) The indicated cell lines were transfected with siRNA against FGFR1 or control siRNA (siCtr). Cells were lysed 5 days after transfection.

(d) NCI-H520 cells were treated with indicated dose of NVP-BGJ398 for 6 hrs. Cell lysates were blotted with phosphorylated and total ERK protein.

(e) The levels of p-ERK were quantified in (D) and are presented as percentage of phosphorylated ERK relative to DMSO treated cells.

(f) Cells were treated with indicated concentration of NVP-BGJ398 for 72 hrs and cell proliferation was shown. Error bars represent mean $\pm$ SD.

(g) Cells were treated with 1μM GDC-0941, 1μM NVP-BGJ398, and combination of these two drugs for 24hrs. Then cells were lysed and blotted with indicated antibodies.

(h) The number of viable cells was determined by Cell Counting Kit and presented as percentage change of cells compared with day 0 (i.e., negative values indicate loss of cells from day 0). Error bars are SD of cells treated n=6.

Figure 4. Co-existing driver mutations in low protein expressing FGFR1 amplified cell lines.

(a, b) Cells were treated with DMSO or 1μM NVP-BGJ398 for 24h, and cell lysates were assessed for levels of phosphorylated RTKs using phospho-RTK arrays. Internal controls at the corner of each membrane allow comparison of phospho-RTK

levels between arrays. Upregulated RTKs are indicated.

Figure 5. Elevated NRG1 expression mitigates the effect of FGFR inhibitor in HCC95 cells

(a) Cells were treated with DMSO or 1μM NVP-BGJ398 for 24h, and cell lysates were assessed for levels of phosphorylated RTKs using phospho-RTK arrays. Internal controls at the corner of each membrane allow comparison of phospho-RTK levels between arrays. Upregulated RTKs are indicated.

(b) HCC95 cells do not have *HER2* amplification. Representative HER2/CEP17 signal pattern is shown. HER2/CEP17 ratio was 0.94.

(c, d) NRG1 is overexpressed in HCC95 cells. (C) mRNA level of NGR1 was determined by quantitative PCR. Fold increase in RNA level was calculated as the ratio of the NRG1 in each cell lines to that of obtained in human fetal lung fibroblast MRC-5 cells. (d) Cells were lysed and blotted with each antibody.

(e, f) Cells were infected with either scramble shRNA vector or two NRG1 shRNA vectors. (e) Cells were lysed after 5 days following shRNA infection and blotted with NRG1 antibody in HCC95 cells. NCI-H520 cells do not express NRG1 and

were used as a negative control. (f) Cell viability was determined by Cell Counting Kit. Error bars are SD of cells treated n=6.

(g) HER3 activation in NCI-H1581 cells following the addition of conditioned medium from HCC95 cells. Cells were added conditioned media and lysted after 60 min.

Figure 6. Inhibition of FGFR with co-existing driver protein enhanced growth suppression and apoptosis induction in FGFR1 amplified cells with low protein expression.

(a) While NCI-H1703 cells were treated with 1μM NVP-BGJ398, 1μM imatinib, or combination of these two drugs, Calu-3 and HCC95 cells were treated with 1μM NVP-BGJ398, 1μM lapatinib, or combination of these two drugs. Drug containing media was replaced at 72 hr treatment. Following five day treatment, plates were stained with crystal violet. A representative plates are shown.

(b) Cells were treated with 1μM of each drug and drug combinations for 24 hrs. Cells were lysed and blotted with indicated antibodies. Asterisk indicates non-specific bands.

Figure 7. Tumors harboring both *FGFR1* gene amplification and protein expression are only a small fraction of *FGFR1* amplified lung SCC and do not have other driver oncogenes.

(a) Results of FGFR1 IHC staining of *FGFR1* gene amplified SCC carcinoma. Gene amplification was defined by FISH analysis.

(b) TCGA data set for RNAseq of 178 lung SCCs were queried for *FGFR1* amplification, *PDGFRa* amplification, FGFR1 mRNA expression and NRG1 mRNA expression. FGFR1 and NRG1 expression was defined as positive when the Z-score of mRNA level was higher than 2.

(c) Proposed treatment strategies for the treatment of *FGFR1* amplified lung SCCs.

Supplementary figure legend

Supplementary Figure S1. *FGFR1* gene is not amplified in NCI-H2444.

Left) *FGFR1* gene copy number was analyzed by Taqman gene copy number assay. Fold increase in copy number was calculated as the ratio of the *FGFR1* signal to that of obtained in human fetal lung fibroblast MRC-5 cells.

Right) Copy number of *FGFR1* measured by FISH. Centromere 8 was co-stained and the ratio of FGFR1 to CEP8 is shown.

Supplementary Figure S2. Protein expression is associated with sensitivity to FGFR inhibitor in *FGFR1* amplified cell line.

(a, b, c) The relationships between FGFR1 protein expression and FISH (a), gene copy number (b), and mRNA (c) are shown.

(d) Cells were categorized based on protein expression and sensitivity to NVP-BGJ398.

Supplementary Figure S3. Absence of CpG island methylation in promoter region of *FGFR1*.

Genomic DNA was extracted by DNeasy Blood and Tissue Kit (QIAGEN) and prepared for methylation analysis with EpiTect Methyl DNA Restriction Kit (QIAGEN). Methylation status of a CpG island in the *FGFR1* promoter was detected using EpiTect Methyl DNA Methylation qPCR Primer Assays from QIAGEN and calculated according to the manufacturer's instruction. Genomic DNA purified from HCT116 cell line genetically lacking methyltransferases (HCT-116-UM) were used as a negative control. In addition, HCT-116 genomic DNA highly methylated by CpG methylase (HCT-116-M) was used as positive control. Both sets of genomic DNA were obtained from Takara Bio Japan.

Supplementary Figure S4. Colo-699N is non-*FGFR1* gene amplified cells.

Left) *FGFR1* gene copy number of Colo-699N cells was analyzed by Taqman gene copy number assay. Fold increase in copy number was calculated as the ratio of the *FGFR1* signal to that of obtained in human fetal lung fibroblast MRC-5 cells.

Right) Copy number of *FGFR1* (2.7) and centromere 8 (2.1) were determined by FISH in Colo-699N cells. The ratio of FGFR1 to CEP8 is shown.

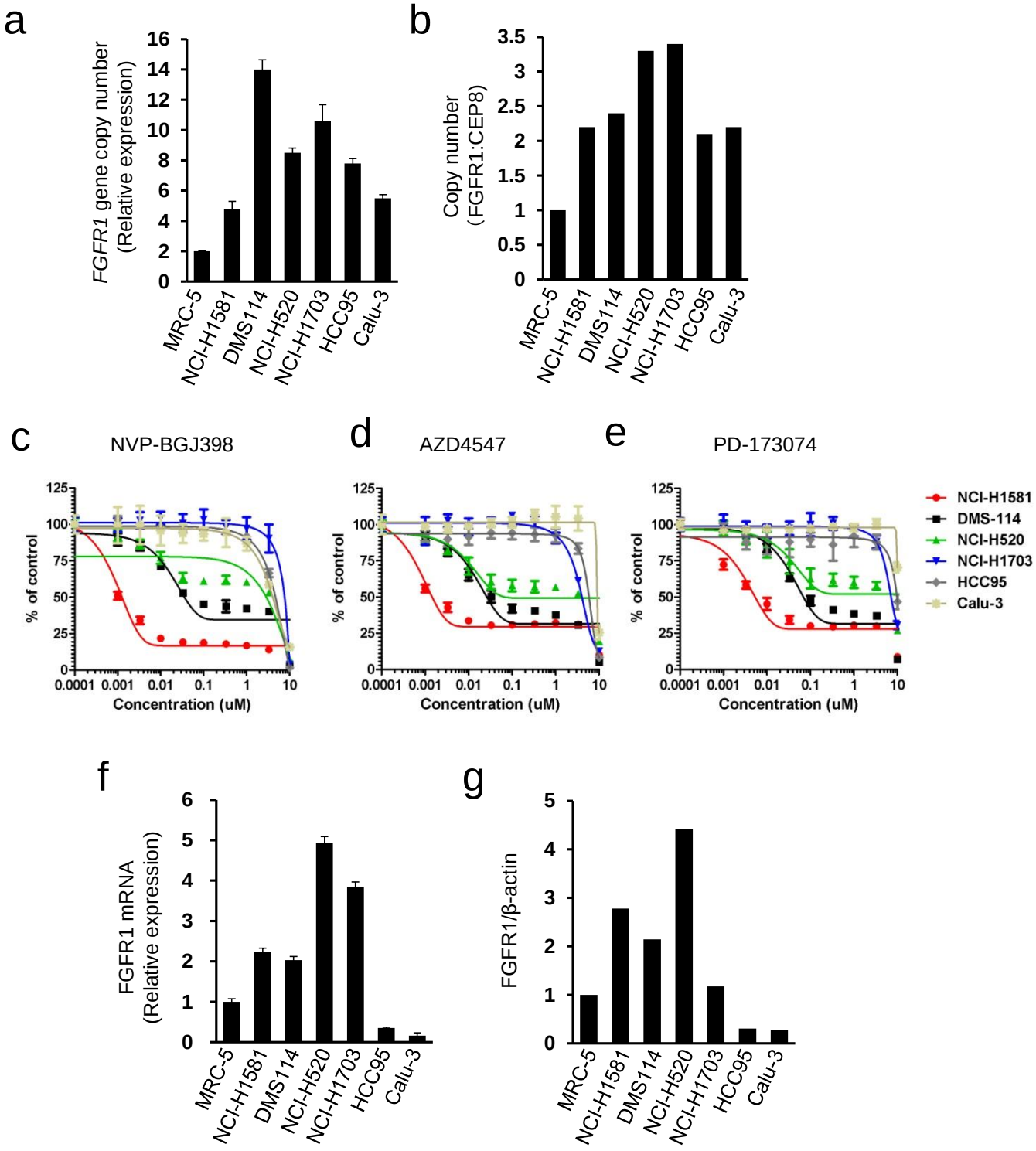
a
FGFR1 gene copy number (Relative expression)
16
14
12
10
8
6
4
2
0
MRC-5
NCI-H1581
DMS114
NCI-H520
NCI-H1703
HCC95
Calu-3
b
Copy number (FGFR1:CEP8)
3.5
3
2.5
2
1.5
1
0.5
0
MRC-5
NCI-H1581
DMS114
NCI-H520
NCI-H1703
HCC95
Calu-3
c
NVP-BGJ398
d
AZD4547
e
PD-173074
% of control
125
100
75
50
25
0
0.0001 0.001 0.01 0.1 1 10
Concentration (uM)
NCI-H1581
DMS-114
NCI-H520
NCI-H1703
HCC95
Calu-3
f
FGFR1 mRNA (Relative expression)
6
5
4
3
2
1
0
MRC-5
NCI-H1581
DMS114
NCI-H520
NCI-H1703
HCC95
Calu-3
g
FGFR1/β-actin
5
4
3
2
1
0
MRC-5
NCI-H1581
DMS114
NCI-H520
NCI-H1703
HCC95
Calu-3

Figure 1

a

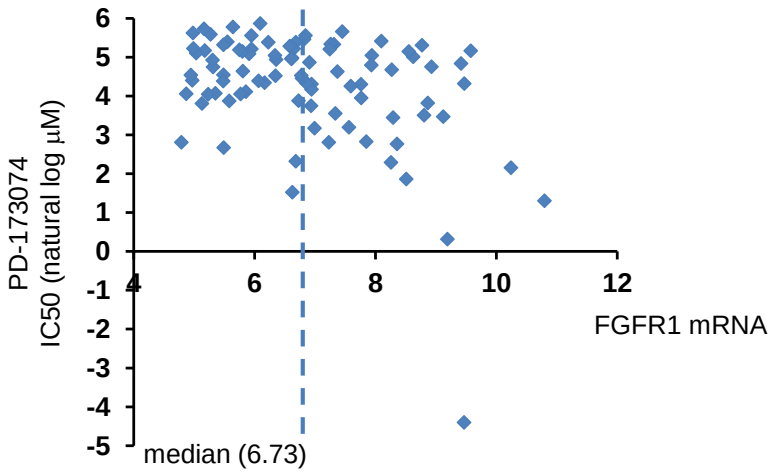

b

	PD-173074		
	sensitive	insensitive	
FGFR1 amplification			
positive	2	4	
negative	0	38	$p < 0.05$

c

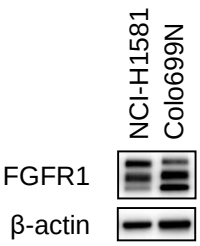

d

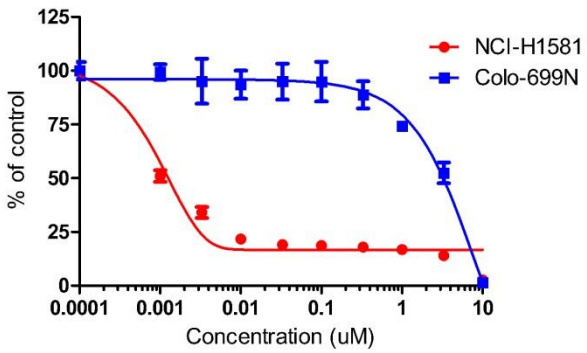

e

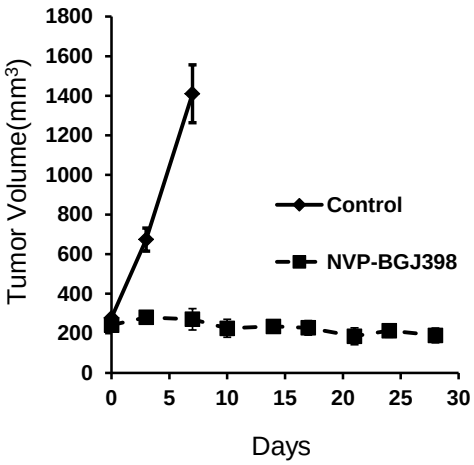

f

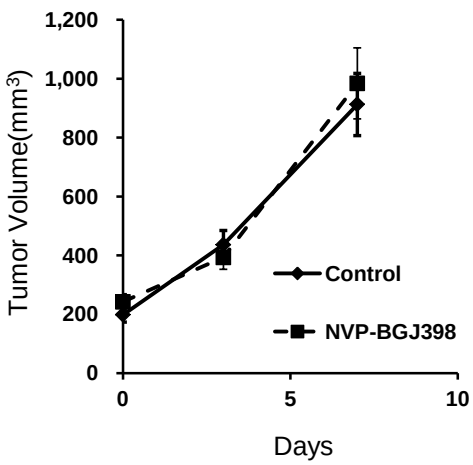

Figure 2

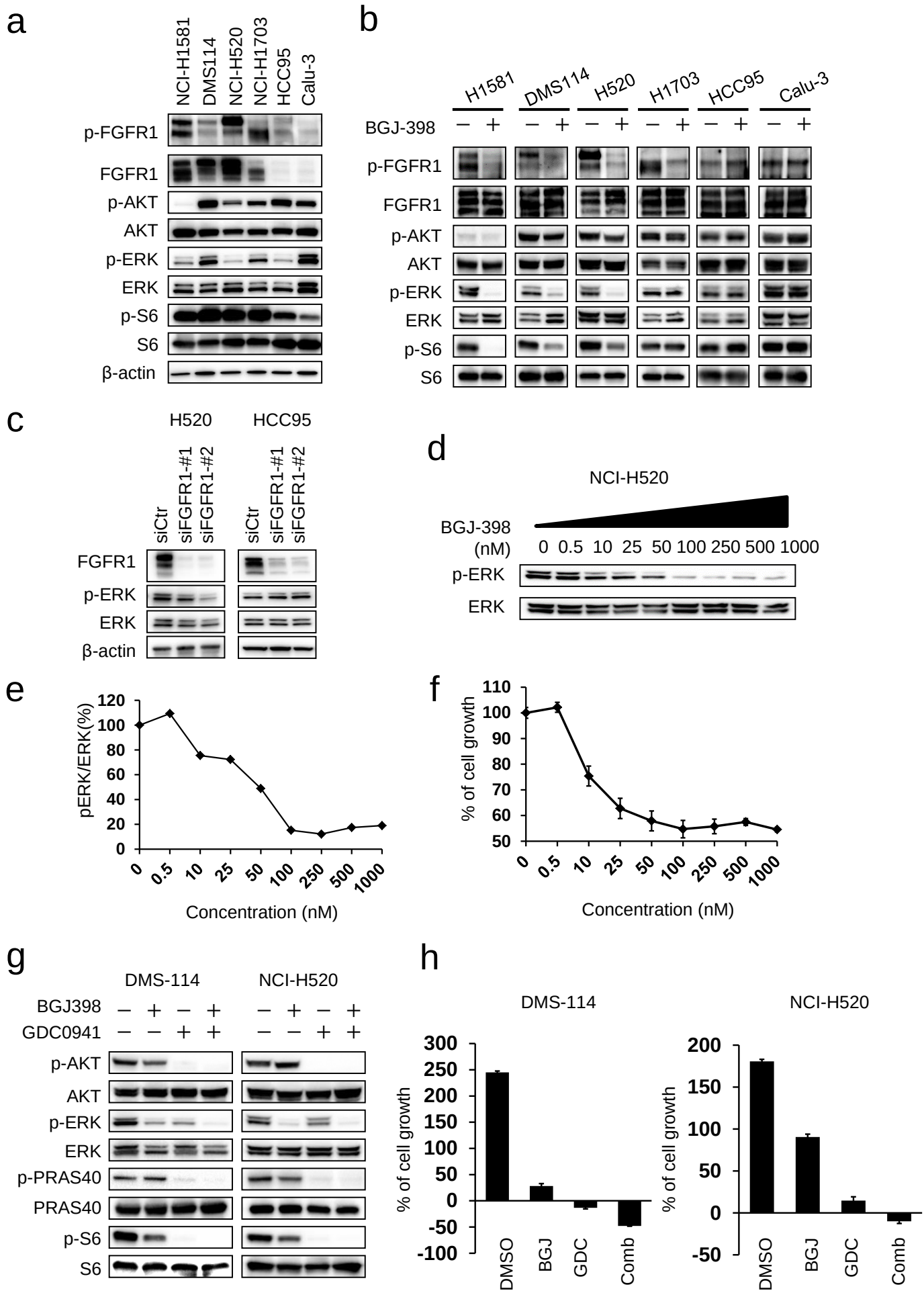
a
NCI-H1581
DMS114
NCI-H520
NCI-H1703
HCC95
Calu-3
p-FGFR1
FGFR1
p-AKT
AKT
p-ERK
ERK
p-S6
S6
β-actin
b
H1581
DMS114
H520
H1703
HCC95
Calu-3
BGJ-398 − + − + − + − + − + − +
p-FGFR1
FGFR1
p-AKT
AKT
p-ERK
ERK
p-S6
S6
c
H520
HCC95
siCtr
siFGFR1-#1
siFGFR1-#2
FGFR1
p-ERK
ERK
β-actin
d
NCI-H520
BGJ-398 (nM)
0 0.5 10 25 50 100 250 500 1000
p-ERK
ERK
e
pERK/ERK(%)
120
100
80
60
40
20
0
0 0.5 10 25 50 100 250 500 1000
Concentration (nM)
f
% of cell growth
110
100
90
80
70
60
50
0 0.5 10 25 50 100 250 500 1000
Concentration (nM)
g
DMS-114
NCI-H520
BGJ398 − + − + − + − +
GDC0941 − − + + − − + +
p-AKT
AKT
p-ERK
ERK
p-PRAS40
PRAS40
p-S6
S6
h
DMS-114
NCI-H520
% of cell growth
300
250
200
150
100
50
0
-50
-100
DMSO
BGJ
GDC
Comb
% of cell growth
200
150
100
50
0
-50
DMSO
BGJ
GDC
Comb

Figure 3

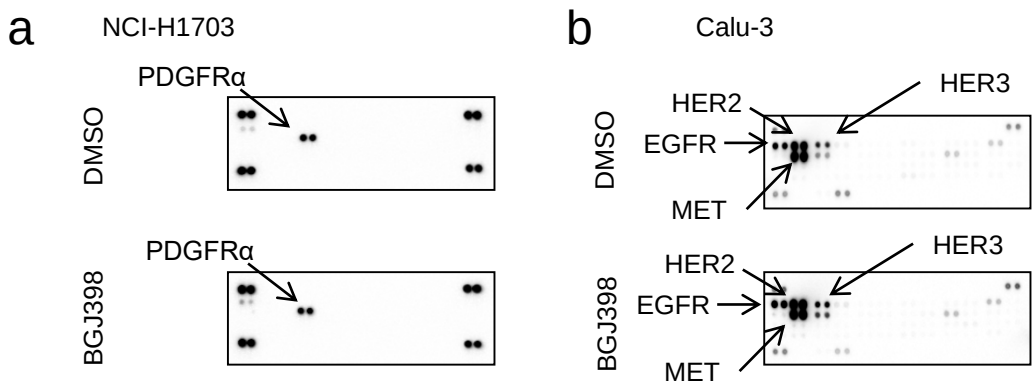
a
NCI-H1703
PDGFRα
DMSO
PDGFRα
BGJ398
b
Calu-3
HER3
HER2
EGFR
MET
DMSO
HER3
HER2
EGFR
MET
BGJ398

Figure 4

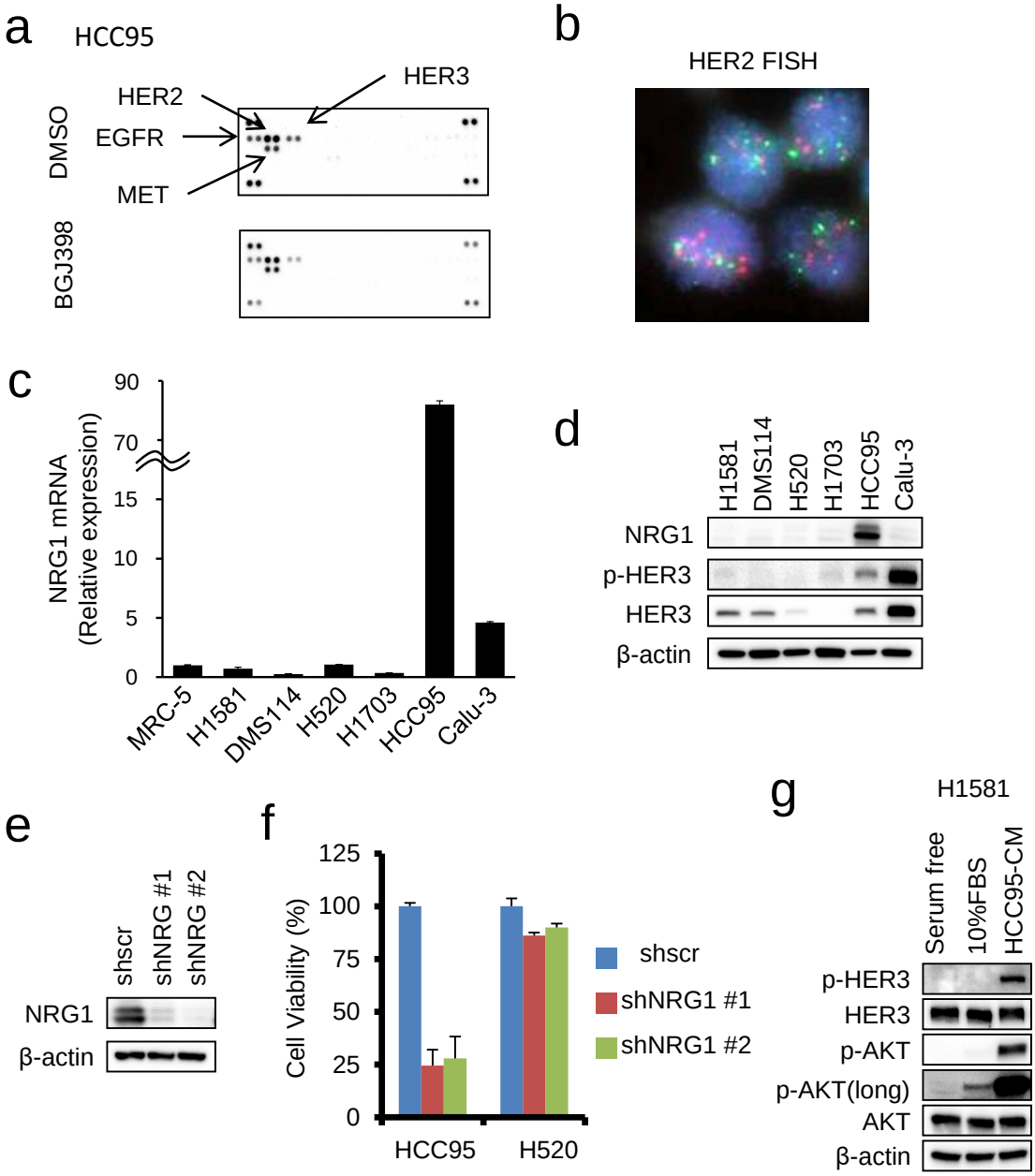
a
HCC95
HER2
HER3
EGFR
MET
DMSO
BGJ398
b
HER2 FISH
c
NRG1 mRNA
(Relative expression)
90
70
15
10
5
0
MRC-5
H1581
DMS114
H520
H1703
HCC95
Calu-3
d
H1581
DMS114
H520
H1703
HCC95
Calu-3
NRG1
p-HER3
HER3
β-actin
e
shscr
shNRG #1
shNRG #2
NRG1
β-actin
f
Cell Viability (%)
125
100
75
50
25
0
HCC95
H520
shscr
shNRG1 #1
shNRG1 #2
g
H1581
Serum free
10%FBS
HCC95-CM
p-HER3
HER3
p-AKT
p-AKT(long)
AKT
β-actin

Figure 5

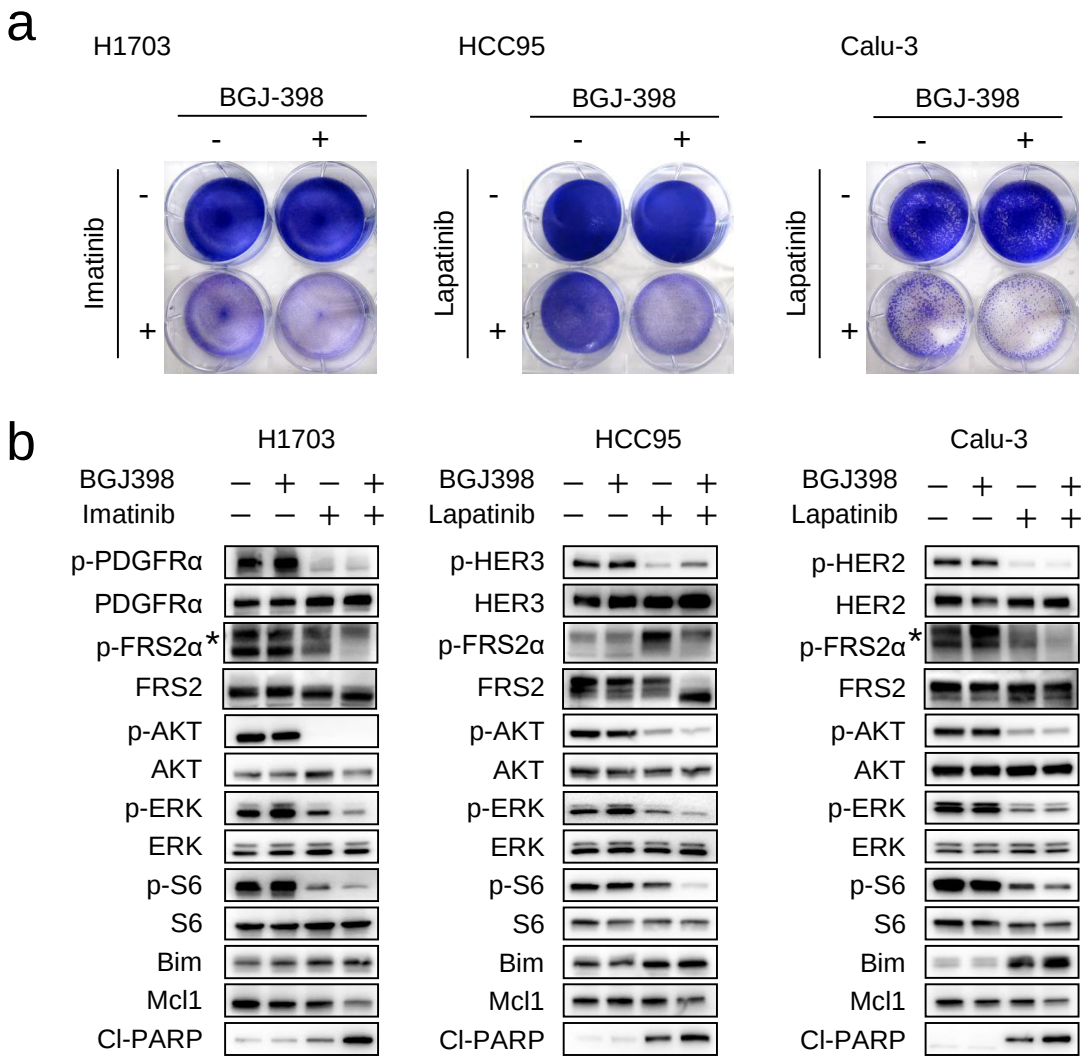
a
H1703
HCC95
Calu-3
BGJ-398
-
+
Imatinib
Lapatinib
b
BGJ398
Imatinib
Lapatinib
p-PDGFRα
PDGFRα
p-FRS2α*
FRS2
p-AKT
AKT
p-ERK
ERK
p-S6
S6
Bim
Mcl1
Cl-PARP
p-HER3
HER3
p-HER2
HER2

Figure 6

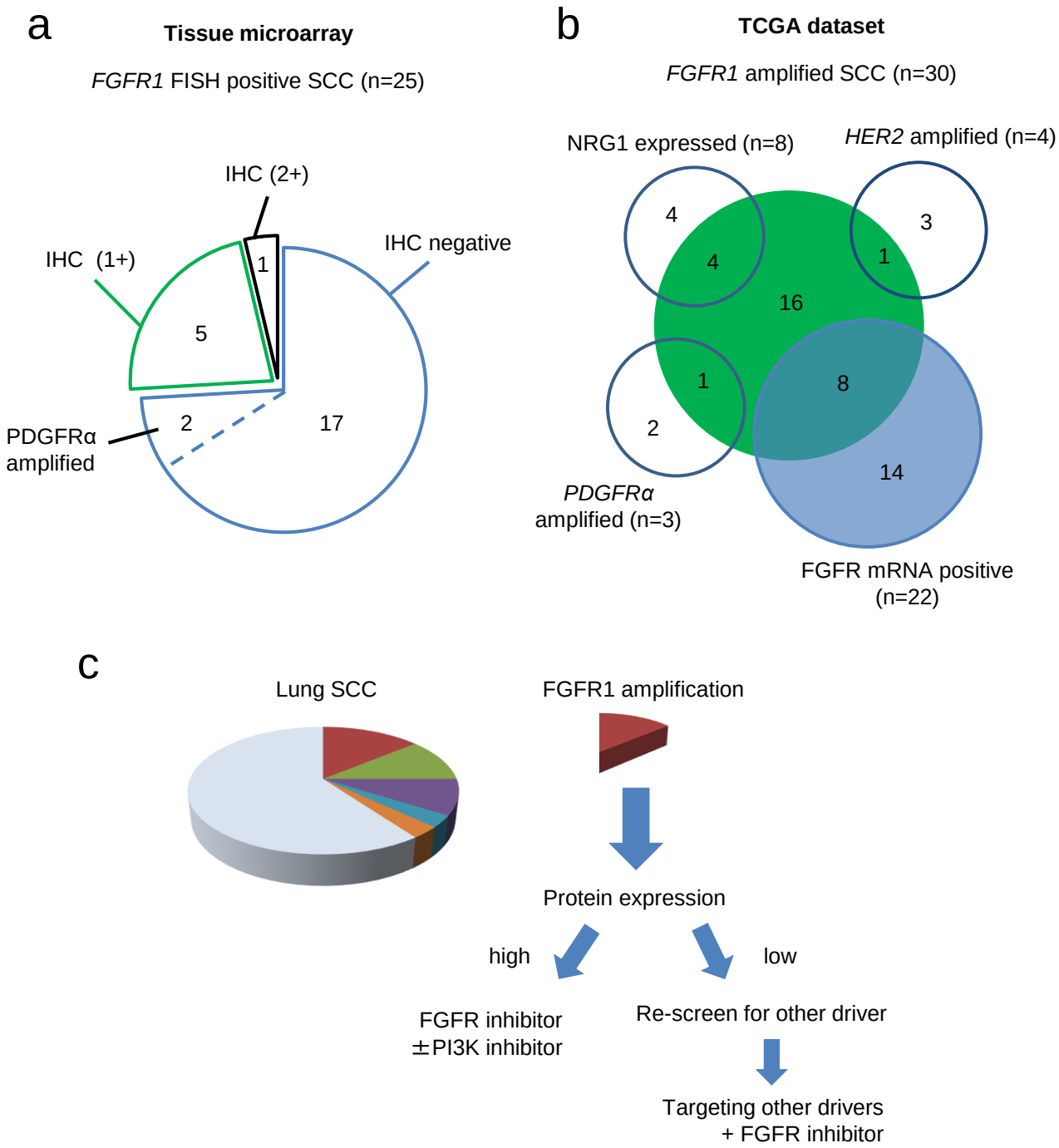
a
Tissue microarray
FGFR1 FISH positive SCC (n=25)
IHC (2+)
IHC (1+)
IHC negative
1
5
2
17
PDGFRα amplified
b
TCGA dataset
FGFR1 amplified SCC (n=30)
NRG1 expressed (n=8)
HER2 amplified (n=4)
4
4
16
3
1
1
8
2
14
PDGFRα amplified (n=3)
FGFR mRNA positive (n=22)
c
Lung SCC
FGFR1 amplification
Protein expression
high
low
FGFR inhibitor ±PI3K inhibitor
Re-screen for other driver
Targeting other drivers + FGFR inhibitor

Figure 7

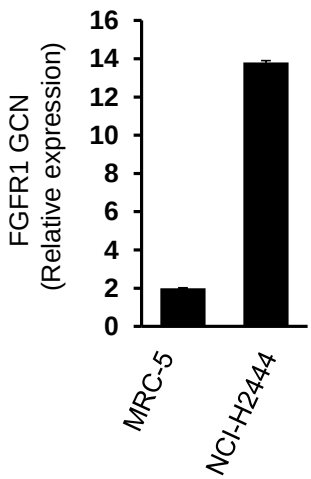

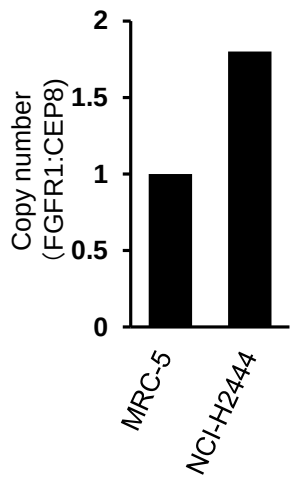

Supplementary Figure S1

a

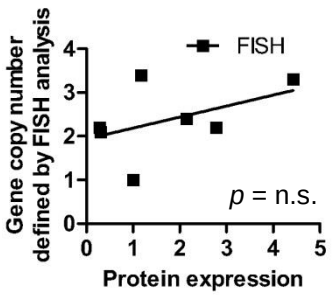

b

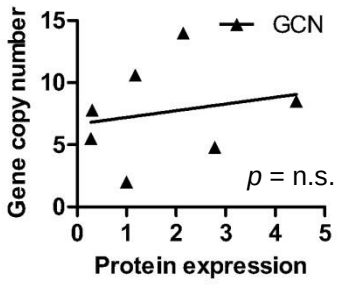

c

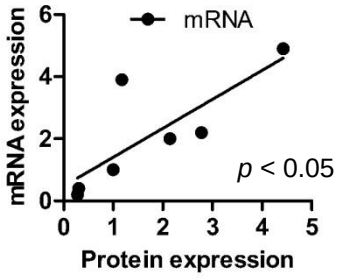

d

		Sensitive (IC50 < 1uM)	Insensitive (IC50 ≥ 1uM)
Protein	High	2	1
	Low	0	3

Supplementary Figure S2

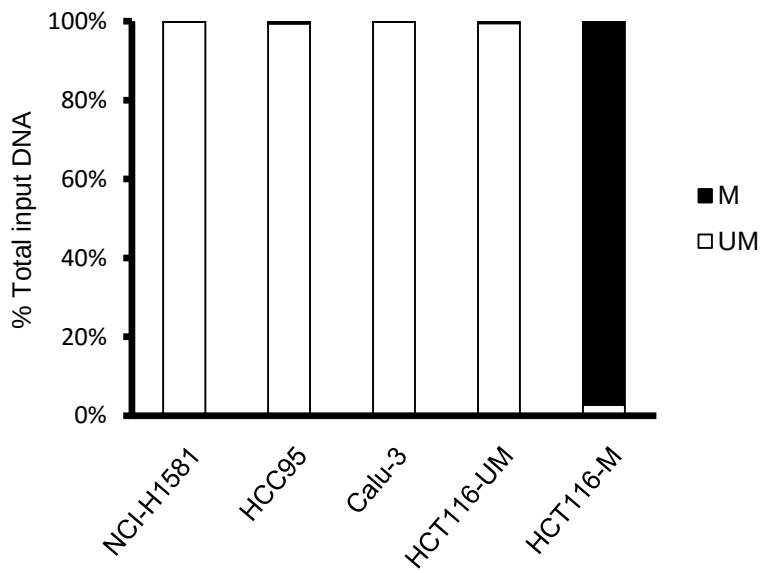

UM : Unmethylated DNA fraction

M : Hypermethylated DNA fraction

Supplementary Figure S3

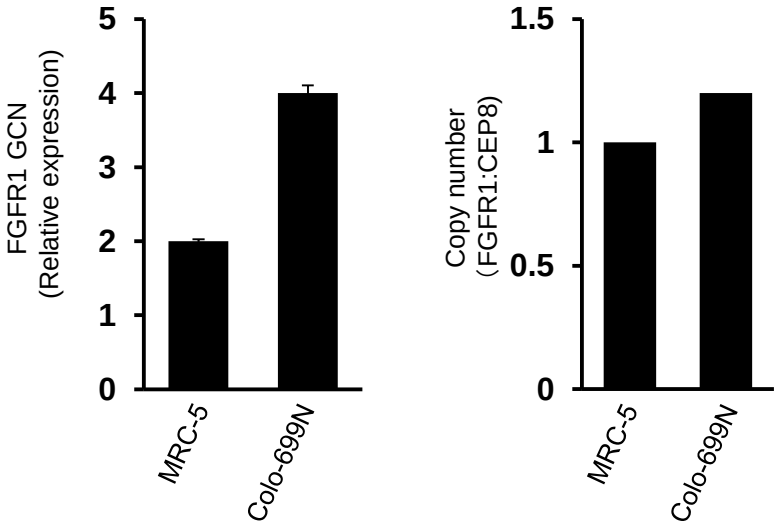

Supplementary Figure S4